Journal of Nuclear Materials 380 (2008) 111–119

Contents lists available at ScienceDirect

Journal of Nuclear Materials

journal homepage: www.elsevier.com/locate/jnucmat

Interaction processes between vacancies and dislocations in molybdenum in the temperature range around 0.3 of the melting temperature

G.I. Zelada-Lambri [a], O.A. Lambri [a,b,*], P.B. Bozzano [c], J.A. García [d], C.A. Celauro [e]

[a] Facultad de Ciencias Exactas, Ingeniería y Agrimensura, Universidad Nacional de Rosario, Laboratorio de Materiales, Escuela de Ingeniería Eléctrica, Avenida Pellegrini 250, 2000 Rosario, Argentina
[b] Instituto de Física Rosario, Member of the CONICET's Research Staff, Argentina
[c] Laboratorio de Microscopia Electrónica, Unidad de Actividad Materiales, Centro Atómico Constituyentes, Comisión Nacional de Energía Atómica, Avenida General Paz 1499, 1650 San Martín, Argentina
[d] Departamento de Física Aplicada II, Facultad de Ciencias y Tecnología, Universidad del País Vasco, Apartado 644, 48080 Bilbao, País Vasco, Spain
[e] Reactor Nuclear RA-4, Facultad de Ciencias Exactas, Ingeniería y Agrimensura, Universidad Nacional de Rosario, Riobamba y Berruti, 2000 Rosario, Argentina

ARTICLE INFO

Article history:
Received 27 March 2008
Accepted 31 July 2008

PACS:
61.50.−f
61.72.−y
62.40.+i
61.16.d
72.15.Eb

ABSTRACT

Mechanical spectroscopy, electrical resistivity and transmission electron microscopy studies have been performed on pre-strained neutron irradiated single crystalline molybdenum in order to check the interaction processes between vacancies and dislocations in the temperature range between room temperature and 1273 K. The anelastic relaxation in molybdenum which appears between 800 K and 1273 K has been separated in two different physical mechanisms depending on the temperature of appearance of the relaxation peak. The physical mechanism which controls the damping peak appearing at around 800 K was related with the dragging of jogs by the dislocation under movement assisted by vacancy diffusion. The damping peak which appears at higher temperatures of about 1000 K was more consistent with the formation and diffusion of vacancies assisted by the dislocation movement.

1. Introduction

The production of electricity from controlled nuclear fusion represents one of the major scientific and technical challenges of the 21st century. Over the past 50 years, the main emphasis of fusion research has been the study of plasmas, the development of plasma theory and pursuit of the technology of magnetic plasma containment. However, over the past three decades, there has been an increasing emphasis on the identification and solution of problems associated with the structural materials, in particular those that will be situated closest to the plasma. The so-called first-wall region of a controlled thermonuclear reactor. A broad range of alloys including austenitic stainless steels, ferritic-martensitic steels, refractory metals and titanium alloys have been investigated in extensive international materials testing programmes in order to identify candidate materials for reactor applications [1].

In particular, molybdenum has a high melting point, a high specific heat, good corrosion, creep resistance and strength at high temperatures. In addition, it has a relatively low thermal neutron cross section. These qualities make molybdenum attractive for the use in the nuclear industry [2].

Nuclear materials are exposed to external stresses and at the same time to irradiation, because of this, it is of great importance to understand the mechanisms of interaction between the defects produced, in order to predict the long-time behaviour of these materials. Several works have been reported in the past 50 years about the radiation damage behaviour in molybdenum and also about its associate recovery stages [3–13].

The temperature range around 0.3 Tm (≈865 K), usually related to stage V of recovery, is particularly interesting in molybdenum due to the strong influence on the mechanical properties both in the pure metal and in technological molybdenum-based alloys. In fact, neutron irradiation in molybdenum at temperatures below 1000 K followed by annealing at temperatures higher than 473 K leads to an increase in the yield stress, the ultimate tensile strength (UTS) and the ductile–brittle transition temperature (DBTT) [8,14]. At annealing temperatures within stage V (>900 K), the yield stress and the UTS begin to decrease.

Mechanical spectroscopy (MS), referred to as the internal friction method (IF) in the early literature, offers unique opportunities to study the mechanical losses due to the interaction, for instance, between dislocation and point defects produced during neutron irradiation in nuclear materials, as molybdenum [15]. The interaction between dislocation and point defects studied by internal

* Corresponding author. Address: Facultad de Ciencias Exactas, Ingeniería y Agrimensura, Universidad Nacional de Rosario, Laboratorio de Materiales, Escuela de Ingeniería Eléctrica, Avenida Pellegrini 250, 2000 Rosario, Argentina. Tel.: +54 341 4802649/4802650x125; fax: +54 341 4821772/4802654.
E-mail address: olambri@fceia.unr.edu.ar (O.A. Lambri).

0022-3115/$ - see front matter © 2008 Elsevier B.V. All rights reserved.
doi:10.1016/j.jnucmat.2008.07.023

friction in molybdenum has been extensively discussed in the 50–450 K temperature range, see for instance Benoit [16] and Seeger [17]. But very little work is done on the internal friction of molybdenum due to the interaction between dislocation and intrinsic point defects above room temperature. Our aim is to study the mechanical losses due to the interaction between dislocations and point defects from room temperature up to near one-third of the melting temperature (0.3 Tm) in deformed and irradiated molybdenum single crystals.

In the previous works [18,19], we found an intense relaxation peak at high temperature for single crystalline samples previously deformed at room temperature. The damping intensity of the peak depends on the degree of plastic deformation and once the peak appeared, after annealing at temperatures above that for vacancy diffusion, the damping values were independent of the amplitude of oscillation. The peak temperature of this relaxation increases with the prior annealing temperature of the sample. However, once the peak stabilises, it has an activation energy of 1.6 eV and 2.7–2.8 eV for peak temperatures of about 800 K and 1000 K, respectively. The activation energy of the relaxation is independent of the crystal orientation.

It has been shown that dislocations are responsible for the relaxation, but also intrinsic point defects as vacancies can be involved. Nevertheless, some open questions remain as: which are the defects involved in the relaxation peak and which mechanism produces these relaxations or energy losses?

In the present work we have studied, using MS, electrical resistivity (ER) measurements and transmission electron microscopy (TEM), the effect of room temperature neutron irradiation on pre-strained samples, with the aim of answering to the above questions and to contribute to the knowledge of the mechanisms, which produce mechanical losses in irradiated and cold-worked molybdenum.

2. Experimental

Twelve single crystals have been used in this work. They were prepared from zone refined single crystal rods of molybdenum in A.E.R.E., Harwell. The residual resistivity of the samples was about 8000, tungsten being the main residual impurity. Samples with the ⟨1 1 0⟩ and ⟨1 4 9⟩ crystallographic tensile axis have been selected to favour the deformation by multiple and single slip, respectively.

The samples used in the mechanical spectroscopy studies were sheets of 20 mm length, 0.2 mm thickness and 2 mm width. In contrast, the samples employed in the electrical resistivity measurements were single-crystal rods of 5 mm diameter and 50 mm length.

Samples were annealed and then deformed in extension at a constant speed of 0.03 cm/min, followed by torsion at room temperature. After the plastic deformation process the samples were irradiated, at room temperature, with neutrons. The status of the samples used is shown in Table 1.

Single crystals, after plastic deformation and mechanical spectroscopy tests, were checked by means of X-rays and metallographical study. Results indicated that the single crystalline state was not changed by the plastic deformation or annealing to the work temperatures.

In the mechanical spectroscopy, MS, measurements, damping (Q^{-1} or internal friction) and natural frequency were measured in an inverted torsion pendulum for free-decaying vibrations, under high vacuum of about 5×10^{-5} Pa; see Ref. [20] for a description of the experimental setup. The maximum strain on the surface of the sample was 5×10^{-5}. The heating and cooling rates employed in the tests were of 1 K/min. A heating and its corresponding cooling run will be called hereafter a thermal cycle. There was no hold time once the maximum temperature had been achieved, during the thermal cycle.

Table 1
Status of the used samples

Sample	Orientation	Elongation (%)	Torsion (%)	Irradiation time (h)
a/sheet	110	3	1	0
b/sheet	110	3	1	10
				10 re-irradiated*
c/sheet	110	3	1	20
d/sheet	149	5	1	0
e/sheet	149	5	1	20
				10 re-irradiated*
f/rod	110	3	1	10
g/rod	149	3	1	10

* Irradiated again after the mechanical spectroscopy measurements, see explanation in the text.

The electrical resistivity, ER, measurements were performed at room temperature by the eddy current decay technique [21]. ER values were measured both before irradiation and after irradiation as a function of the annealing temperature. Annealing treatments were performed by heating the sample at a rate of 1 K/min under pure argon at normal pressure followed by cooling into the furnace, under the same protective atmosphere.

For transmission electron microscopy, TEM, examinations, thin foils were prepared with the double jet technique using 12% H_2SO_4 in methyl alcohol. Observations were carried out in a Phillips CM200 transmission electron microscope with an energy dispersive X-ray spectrometer EDAX DX-4, operated at 200 kV.

Low flux neutron irradiation was performed at room temperature, at the Siemens SUR 100 nuclear reactor, RA-4, of the National University of Rosario – National Atomic Energy Commission of Argentina. The RA-4 was operated at 0.7 W. Samples were positioned in the horizontal channel, which passes through the reactor core inside of a cylinder of poly-methyl-methacrylate (PMMA) of 250 mm length and 25 mm diameter, with a wall and a bases thickness of 2 mm and 20 mm, respectively. The fluxes of thermal, epithermal and fast neutrons at the position where the samples were placed were 5.7×10^{11} n/m^2 s, 8.1×10^{9} n/m^2 s and 5.0×10^{11} n/m^2 s, respectively. The energy of the thermal neutrons was about 0.025 eV. Epithermal and fast neutrons had averaged energies of 50 KeV and 0.8 MeV, respectively. Taking into account the previous reported works [13,22], an estimation of the irradiation dose in dpa (displacement per atom) less than 1×10^{-5} could be done.

Considering that the maximum energy transfer, E, for a neutron of mass m and kinetic energy, E_o, emitting a lattice atom of molybdenum of mass M is [23,24]

$$E = \frac{4\,\mathrm{mM}}{(m+M)^2} E_o \tag{1}$$

we have calculated the number of displacements through the Kinchin–Pease model for hard sphere collisions [23], such that

$$\text{Number of displacements} = \frac{E}{2E_d} \tag{2}$$

where E is the transferred energy (56 KeV, according to Eq. (1)) to the primary knock atom corresponding to fast neutron damage (with $E_o = 0.8$ MeV) and E_d is the displacement threshold energy for molybdenum ($E_d = 37$ eV [25]). A value of 800 displacements was obtained. It is convenient to mention that the number of displacements calculated from the Kinchin–Pease model is a maximum limit attained for a temperature of 0 K, where recombination of defects does not occur. In addition, around 600 displacements are obtained if Eq. (2) is multiplied by 0.8, corresponding to the modified Kinchin–Pease model which takes into

account the recombination of defects at temperatures higher than 0 K [25].

On the other hand, considering the energy transferred to the primary knock atom, given in Eq. (1), and the displacement threshold energy used for the Kinchin–Pease model, we have made an estimation of the full cascade of displacements promoted by the neutron irradiation employing SRIM 2006.02 (formerly called TRIM) software [26]. The displacements, replacements, vacancies and interstitials produced by each atom in movement owing to the neutron impact were calculated, i.e. the damage done to the target from recoil cascades. SRIM was used under the mode the so-called type of calculus for damage cascade for neutrons, etc., using TRIM.dat external file. Different input files (TRIM.dat) were made containing up to 19 atoms in different positions in the bcc lattice and different orientations of incident neutrons in such a way of describing a random irradiation event. The averaged results calculated per atom for incident neutrons with 0.8 MeV, which correspond to the energies transferred to the primary knock atom of 56 KeV according to Eq. (1), were: displacements: 700, replacements: 50, vacancies: 650, and interstitials: 664. These calculations result in a reasonable agreement with the Kinchin–Pease results.

An estimation of the amount of vacancies promoted in the samples during 10 hours irradiation would be around 5×10^{14}, which gives rise to a vacancy concentration of about 5 ppm. This amount of vacancies and its evolution with temperature will be enough for being detected through MS and ER measurements, as it will be discussed in Section 4.

3. Results

3.1. Dependence of the internal friction relaxation on plastic deformation and irradiation

Fig. 1 shows the damping spectra measured in a deformed sample (a) detailed in Table 1. During the first heating, after the room temperature deformation, the sample showed an increasing background with temperature. Nevertheless, on cooling a well developed internal friction peak was present (peak marked A in Fig. 1). The peak height and temperature are very reproducible for samples of the same type, but they are strongly dependent both on the orientation and on the plastic deformation degree. See Refs. [18,19] for details.

The behaviour of the peak on consecutive warm-ups has been previously reported [18,19]. The peak moves to a slightly higher temperature and increases in intensity on consecutive heating to 973 K, but then stabilises at a peak temperature of around 800 K (see peak B in Fig. 1). When the maximum annealing temperature, during the thermal cycles, is increased to 1250 K, the peak temperature changes to around 1000 K (peak C in Fig. 1). Further runs to 1250 K decrease the intensity of the peak and it disappears if the sample keeps vibrating for a long time at 1250 K. When the maximum temperature of the thermal cycles was increased in smaller steps, the shifting in the peak temperature varied progressively as the temperature in the test increased [19].

Samples (b) and (c), which were prepared from the same rod of sample (a) and under the same thermomechanical conditions, were deformed and then irradiated for 10 and 20 h, respectively, see Table 1. Fig. 2 presents the results for sample (b). In the first heating, sample (b) shows an increasing background with temperature, but on cooling the internal friction peak appears (peak marked A in Fig. 2). In this case, the peak appears at a lower temperature and has a smaller intensity than the one for non-irradiated samples. Annealing up to 973 K produces a slight increase both in the peak temperature and in the peak height. Successive thermal cycles up to 1073 K stabilise the peak at around 800 K (peak marked B in Fig. 2). The temperature of the relaxation is very similar to that of the non-irradiated samples, but is less intense. Further increase in the temperature of annealing up to 1250 K leads to a strong shift in the peak temperature and to a decrease in the peak height, in a similar mode than for the non-irradiated sample (see peak marked C in Fig. 2).

The damping peak for sample (c) after 20 h irradiation can be seen in Fig. 3. The peak appears at a lower temperature and has

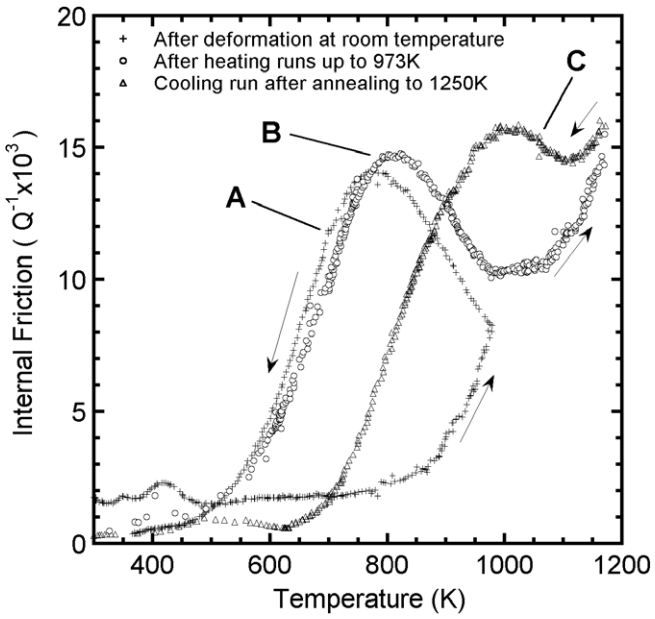

Fig. 1. Damping spectra measured for a sample of type (a) during different heating runs. (A) After deformation at room temperature. (B) Stable spectrum after heating runs up to 973 K. (C) Spectrum corresponds to a cooling run after annealing to 1250 K performed during a previous thermal cycle. Arrows indicate the warming and cooling runs.

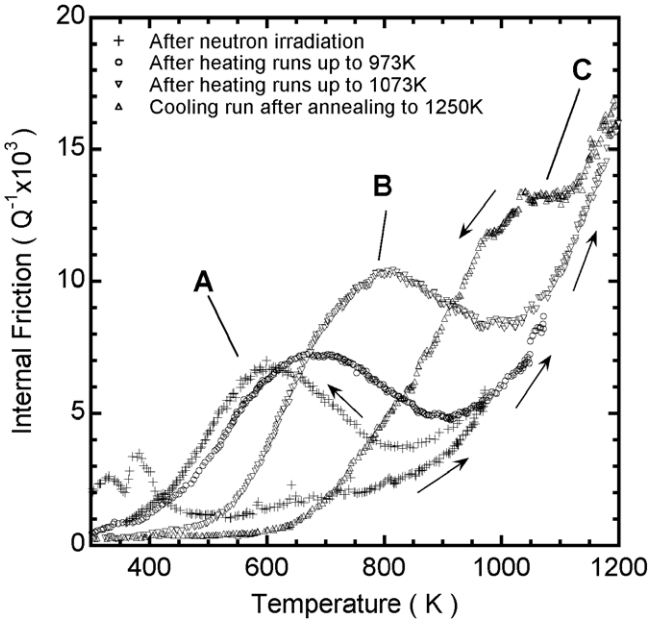

Fig. 2. Damping spectra measured for a sample of type (b) during different heating runs. (A) After neutron irradiation. (B) Stable spectrum after heating runs up to 1073 K. (C) Spectrum corresponds to a cooling run after annealing to 1250 K performed during a previous thermal cycle. Arrows indicate the warming and cooling runs.

a smaller intensity than the one for non-irradiated samples. The behaviour of the peak after the successive thermal cycles is completely similar to that exhibited for sample (b), irradiated for 10 h, although in this case the peak presents a final lower intensity due mainly to the decrease in the damping background.

Samples (d) and (e) oriented for single slip were cut from the same ingot and prepared in the same manner, then deformed and one of them, sample (e), was irradiated for 20 h. Fig. 4 shows the results for the deformed (crosses) and deformed plus irradiated sample (circles). During the first heating, after the room temperature deformation, sample (d) showed an increasing background with temperature. As in the other cases, on cooling a well developed internal friction peak was present (peak marked A in Fig. 4). The irradiated sample presents similar behaviour (peak marked B in Fig. 4). As can be seen in the figure, the peak height and temperature change very little after irradiation. The influence of irradiation in this sample is to decrease the height of the peak slightly and to move it to a little higher temperature.

3.2. The effect of the re-irradiation

The damping peak in sample (b) practically disappears when the sample is vibrated for a few hours at 1250 K. A new 10 h re-irradiation at room temperature and subsequent annealing, during the thermal cycles, restores the peak. This behaviour can be observed in Fig. 5. This figure shows the internal friction spectrum for the sample (b) after a few hours vibrating at 1250 K (spectrum marked A in the figure). In the warming run just after re-irradiation, the γ relaxation at 440 K and a damping increase starting between 500 and 550 K are observed, but the peak is absent. In the cooling run after the sample has been heated to 973 K, the peak is again restored (spectrum B in Fig. 5). Further annealing to higher temperatures displaces the peak to around 1000 K, spectrum marked C on cooling in the same figure. Similar behaviour in a re-irradiated ⟨149⟩ sample (e), in Table 1, was found.

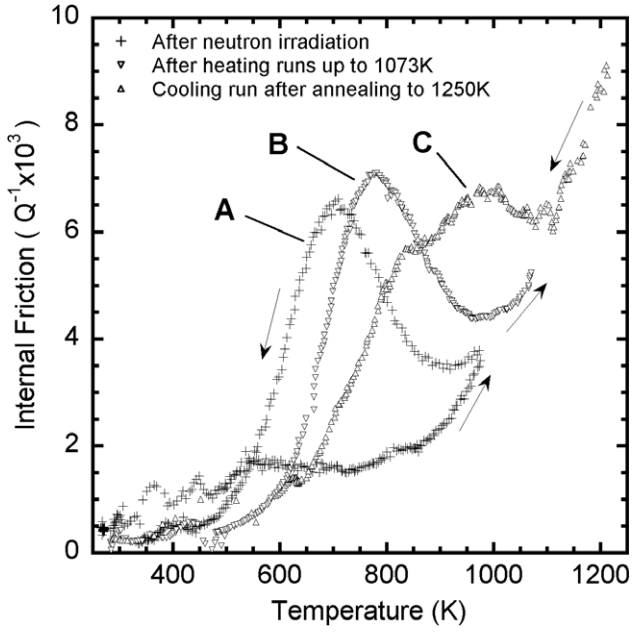

Fig. 3. Damping spectra measured for a sample of type (c) during different heating runs. (A) After neutron irradiation. (B) Stable spectrum after heating runs up to 1073 K. (C) Spectrum corresponds to a cooling run after annealing to 1250 K performed during a previous thermal cycle. Arrows indicate as in previous figures.

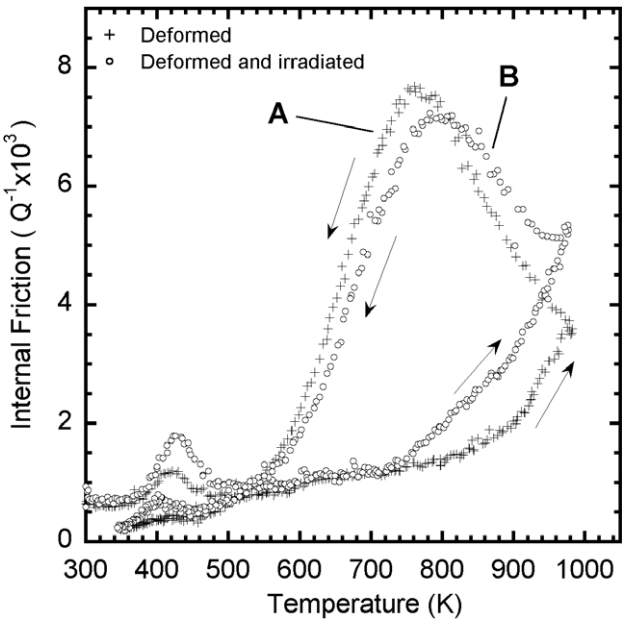

Fig. 4. Damping spectra for ⟨149⟩ samples. (A) Sample (d) deformed, and (B) sample (e) deformed and irradiated. Arrows mean as in previous figures.

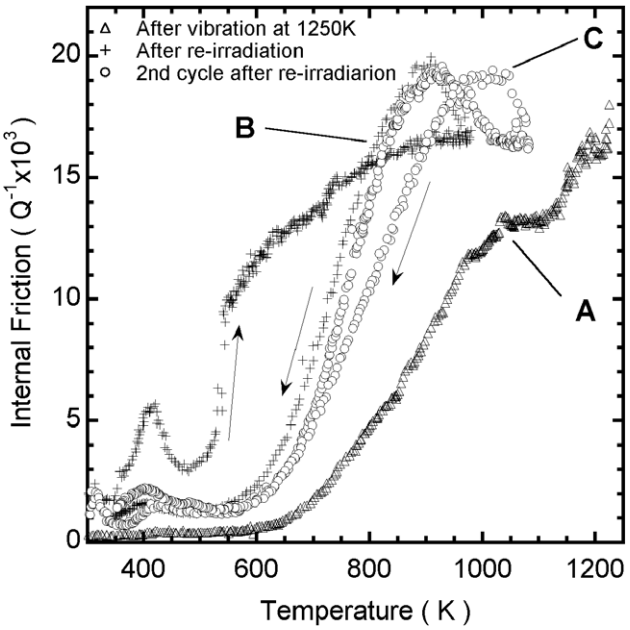

Fig. 5. (A) Spectrum for a sample (b) after vibration several hours at 1250 K. (B) Peak during cooling in the first thermal cycle after the re-irradiation with neutrons. (C) Peak during cooling in the second thermal cycle after the re-irradiation. Arrows mean as in previous figures.

3.3. Electrical resistivity measurements

We measured the electrical resistivity of two irradiated samples of different orientations as a function of the annealing temperature, samples (f) and (g) in Table 1. Results are shown in Fig. 6 for both the (f, ⟨110⟩) and (g, ⟨149⟩) samples by means of full symbols. Empty symbols indicate the value of the ER before the neutron irradiation.

The ER increases, as the annealing temperature is increased, up to a maximum. This is observed at around 600 K for both kinds of samples. At higher temperatures, the ER curves begin to decrease.

In the curve corresponding to sample (f) a stage around 1000 K appears. In contrast, for sample (g) this stage cannot be clearly distinguished.

3.4. Transmission electron microscopy results

The dislocation structure of deformed molybdenum has been studied by (TEM) in the previous works [27–31]. Samples deformed at room temperature in the deformation range used in this work show screw dislocations with a high density of jogs but few edge dislocations. However, dislocation fragments with Burgers vectors a⟨100⟩ and prismatic loops were present.

Nevertheless, with the aim of checking the dislocation arrangement that results after annealing during the thermal cycles in the MS measurements, we have performed TEM studies on the same samples explored by means of MS. Fig. 7(a) shows the micrograph for a sample of type (d), which presented a damping value of about 10×10^{-3} at 980 K. Fig. 7(b) shows a magnification of a zone of Fig. 7(a). Fig. 8(a) shows the micrograph for a sample of type (a). Prior to TEM examinations, the sample showed a damping value of about 17×10^{-3} at 900 K. A magnification of a zone of Fig. 8(a) is shown in Fig. 8(b).

As it can be seen in Figs. 7 and 8, after annealing during the MS test the dislocations are more jogged in ⟨110⟩ samples than in ⟨149⟩ samples. In addition, the dislocation density, determined by counting the dislocation lines, is larger in ⟨110⟩ sample than in the ⟨149⟩, in agreement with the multiple slip condition for ⟨110⟩ sample. The character of the dislocations in the above figures is mixed, i.e. the dislocations have both screw and edge components. An analysis of constructive interference allowed us to relate the (110) plane as the sliding one and the Burgers vectors with the ⟨111⟩ direction.

Fig. 9(a) shows the micrograph for a re-irradiated sample of type (b), after few hours of vibration at high temperature in the MS test. Prior to re-irradiation, the sample showed spectrum A, which is depicted in Fig. 5.

A smaller dislocation density is found for this type of sample as a consequence of the dislocation recovery during the MS thermal cycles, which is in agreement with the strong decrease in intensity of the damping peak, at around 1000 K. The same characteristics as above for the sliding plane and Burgers vector was found out for this type of sample.

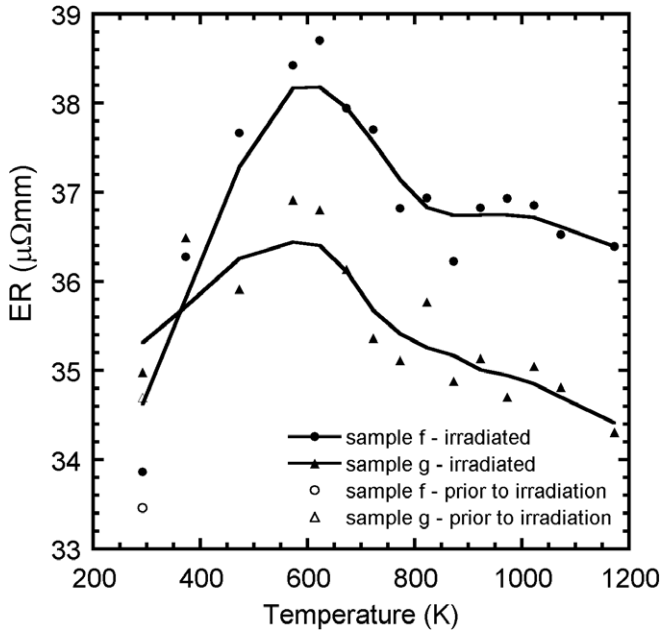

Fig. 6. Behaviour of the electrical resistivity at room temperature as a function of the annealing temperature, full points. Empty points, ER values prior to irradiation. Sample (f), circles. Sample (g), triangles.

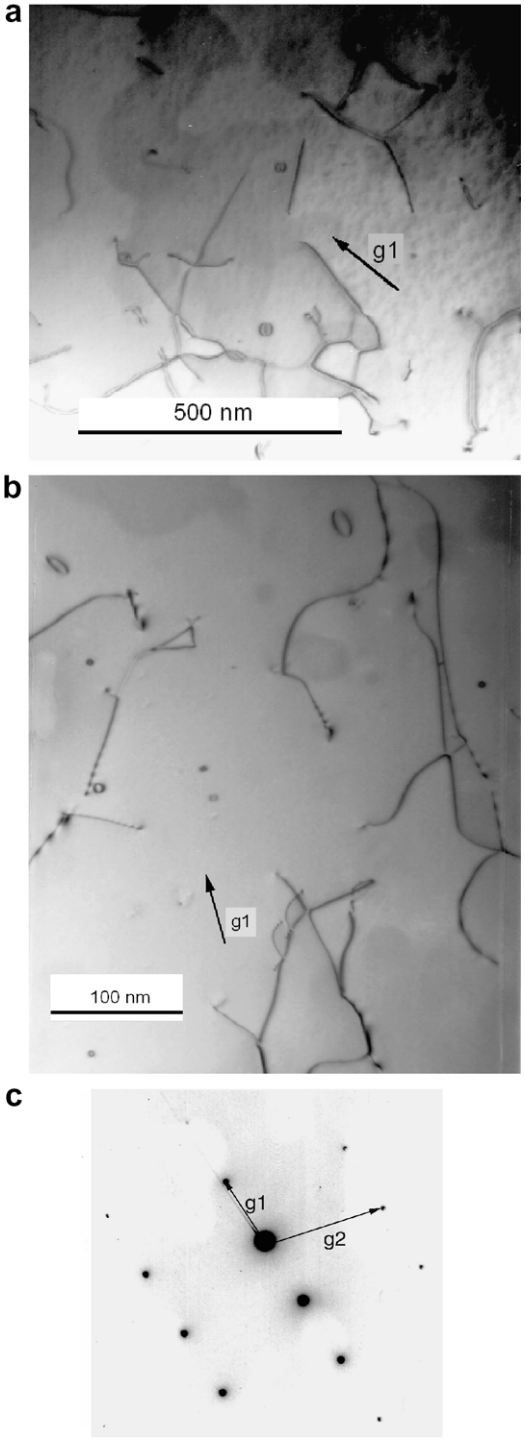

Fig. 7. (a) TEM Micrographs for a sample of (d) type, (b) zoom of a zone, (c) selected area diffraction pattern: $g1 = (-1,1,0)$, $g2 = (-2,-1,1)$, zone axis [1,1,3].

4. Discussion

The effect of irradiation on the samples is to increase the number of intrinsic point defects, vacancy mainly, because interstitials are mobile at lower temperatures than room temperature [32,33].

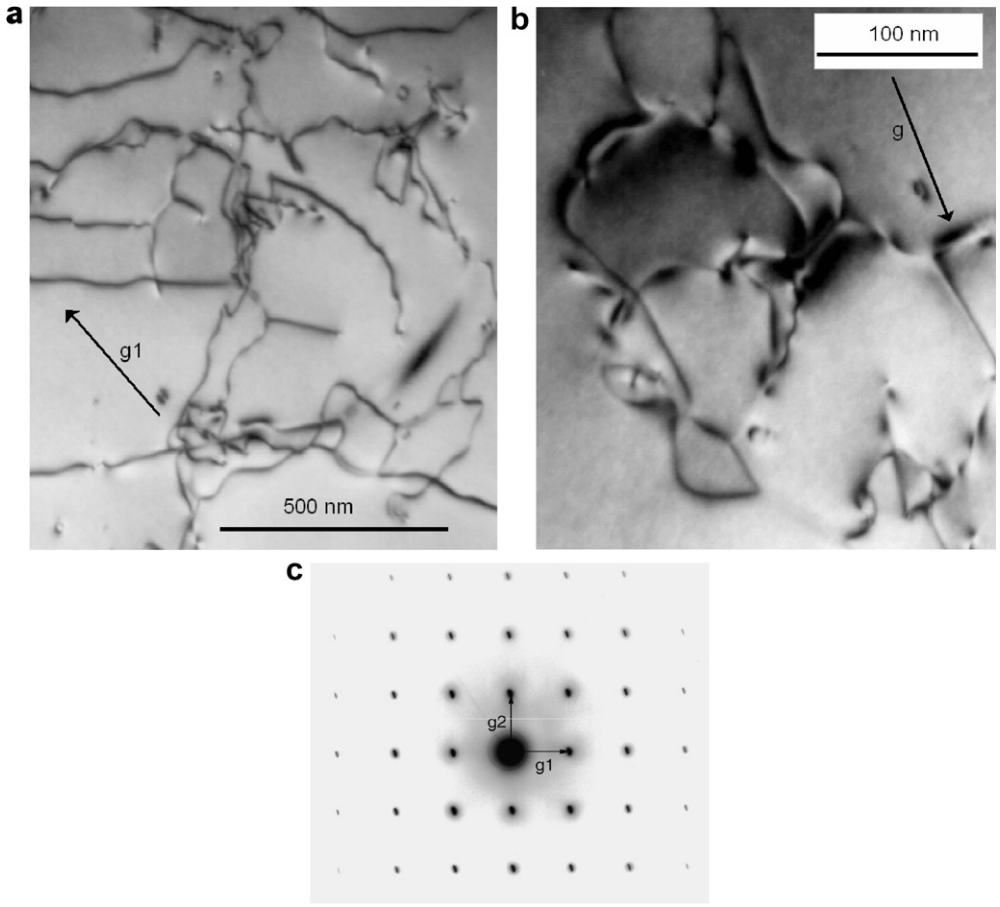

Fig. 8. (a) TEM Micrographs for a sample of (a) type, (b) zoom of a zone, (c) selected area diffraction pattern: $g1 = (-1,-1,0)$, $g2 = (1,-1,0)$, zone axis $[0,0,1]$.

After irradiation, dislocations are pinned producing a decrease in the internal friction background [34], see Figs. 1–3. In addition, samples ⟨110⟩ are more sensitive to irradiation than ⟨149⟩, as it is revealed by the behaviour of the damping shown in Figs. 1–4. In fact, the effect of irradiation in ⟨110⟩ samples is to reduce the damping peak and to move it to lower temperatures. In contrast, in samples oriented for single slip the irradiation after deformation does not produce clear changes.

The difference in the MS behaviours for irradiated ⟨110⟩ and ⟨149⟩ samples can be related to different dislocation arrangements in each type of deformed single crystal. Indeed, samples oriented for multiple slip have more active slip systems and present higher density of dislocation, more jogged and shorter dislocations than the ⟨149⟩ samples, as it was observed by TEM as shown in Figs. 7 and 8.

It should be mentioned that the behaviour of the damping response in the MS tests are in agreement with that exhibited by the ER curves, Fig. 6. In fact, the increase in the ER values from 300 K up to 600 K in both ⟨110⟩ and ⟨149⟩ samples coincides with stage III in irradiated samples, which was related to the movement of vacancies [8,10]. It has been reported that in neutron irradiated molybdenum at room temperature, a subsequent annealing at temperatures between 473 K and 573 K produces an increase in the yield stress and in the UTS [8], which result in agreement with our ER results in low flux irradiated molybdenum. Consequently, within the temperature range of stage III, the appearance of internal stresses can be assumed, which lead to the increase in the ER reported in Fig. 6 [35]. Therefore, the appearance of internal stresses in stage III, due to the reorganization of the defects out of thermodynamic equilibrium, leads to the locking of dislocations during the first run-up in temperature in the MS test, see Figs. 1–3. It gives rise to the amplitude-dependent damping background without the appearance of the damping peak. In contrast, on increasing the annealing temperature to 973 K (stage V), which is higher than the temperature for the maximum observed in the ER curves, the vacancies move to the dislocations and in the cooling down the damping peak appears, without dependence with the amplitude of vibration.

Moreover, thermal cycles in irradiated samples up to higher temperatures (1223 K) lead to a strong shift in the peak temperature and to a decrease in the peak intensity, which are similar to unirradiated samples, in agreement with a larger temperature for the recovery of the radiation damage effects [10,14].

On the other hand, it can be seen in Figs. 2 and 3 that during the heating runs up to 1250 K, the irradiated samples presented a peak (labelled C in figures) which is composed of more than one elementary relaxation. Fig. 10 shows this damping peak after the background subtraction for sample (c), irradiated for 20 h, together with peak marked B in Fig. 3. Certainly, the peak labelled C is composed of at least two relaxations at around 800 K and 1000 K, as can be clearly distinguished in the figure.

In the previous works, we showed that the spectrum of deformed molybdenum exhibited a damping peak that for different final annealing temperatures appears in the range 800–1000 K [18,19]. The activation energy we measured varied depending on the peak position, although the activation energy obtained for the peak stabilised at around 800 K, hereafter called LTP, was 1.6 eV, and it was 2.7–2.8 eV for the peak stabilised at 1000 K, hereafter called HTP [19]. Consequently, the LTP could be due to the exhausting of the vacancies produced by the deformation when

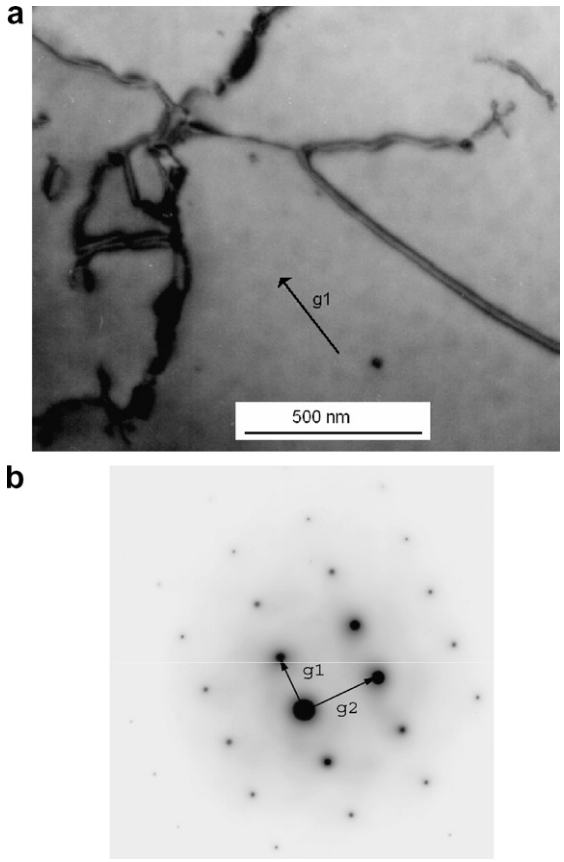

Fig. 9. (a) TEM Micrograph for a sample of (b) type after re-irradiation after the A spectrum in Fig. 5 (see explanation in the text), (b) selected area diffraction pattern: $g1 = (-1,0,1)$, $g2 = (0,-2,0)$, zone axis $[1,0,1]$.

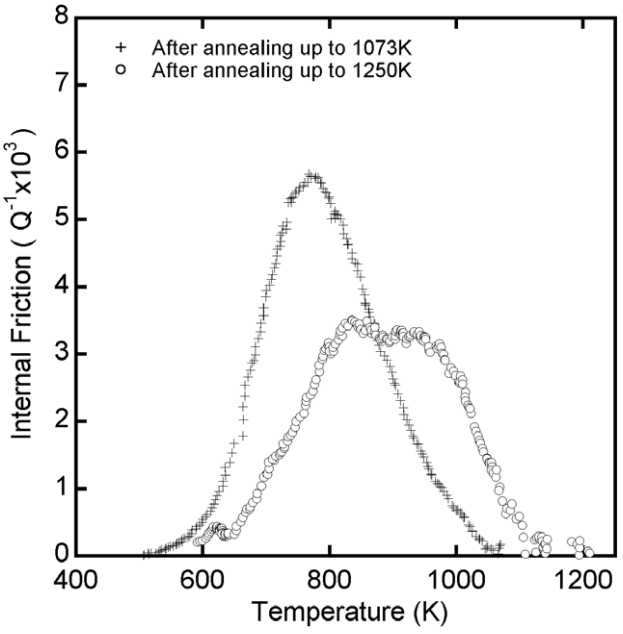

Fig. 10. Peaks obtained for a sample of (c) type. Circles: after the background subtraction, from C curve in Fig. 3 (after annealing up to 1250 K). Crosses: after background subtraction from B curve in Fig. 3 (after annealing up to 1073 K).

the sample is annealed and the HTP could be related to the creation of vacancies at higher temperatures. Indeed, the extra amount of vacancies produced by irradiation in the deformed samples allows us to observe the two relaxations, at least once, in the same spectrum (curves C in Figs. 2 and 3).

The splitting in two different relaxation processes, i.e. LTP and HTP, results in agreement with a previously reported theoretical study [36].

Peak temperatures and frequencies data for LTP and HTP peaks for irradiated samples fit very well in the Arrhenius plot performed by us to calculate the activation energy, H, of the peaks for deformed samples [19], Fig. 11. In Fig. 11, the empty circles and the square represent the peaks corresponding to the LTP and HTP, respectively, of irradiated samples presented in the work. Therefore, it can be proposed that the same physical mechanism is controlling the LTP ($H = 1.6$ eV) and HTP ($H = 2.7$ eV) peaks in both irradiated and non-irradiated samples. The difference in the peak temperature and intensity should be related only to a different arrangement of defects on the dislocation lines.

It should be stressed that re-irradiation clearly demonstrates that the interaction of vacancies with dislocations is the mechanism responsible for the relaxation that appears in deformed and annealed samples and which stabilises at around 800 K, the LTP. Indeed, deformed samples present the peak after annealing in the cooling run. In a previous work, we showed that when the relaxation practically disappears after the sample is vibrated for a few hours at 1250 K, a new deformation (5% torsion) restores the peak in the cooling run after annealing [18]. In the re-irradiated sample, see Fig. 5, the peak is again restored in the cooling run after the sample was re-irradiated and heated to 973 K, but the sample was not deformed. Here, the vacancies produced after irradiation migrate during annealing to the dislocations which remains of the previous deformation and restores the peak. As it can be seen from the micrograph in Fig. 9, the initial dislocation density has decreased due to the recovery of the structure during the successive thermal cycles at 1250 K.

The peak promoted by re-irradiation is also in agreement with the Arrhenius plot as shown in Fig. 11. In this figure, the value for the peak measured in the re-irradiated sample (b) is plotted

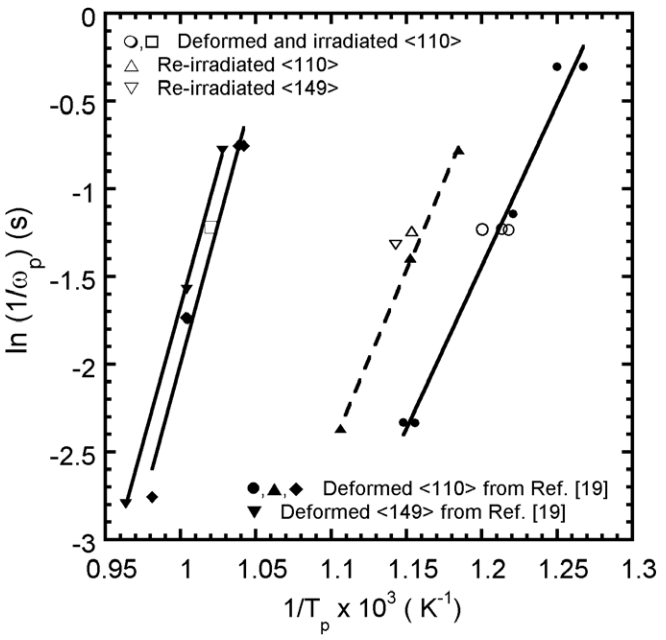

Fig. 11. Full symbols and straight-lines correspond to the Arrhenius plot for deformed molybdenum, taken from Ref. [19]. Empty circles and squares correspond to samples oriented ⟨110⟩ deformed and irradiated. Empty triangle corresponds to a re-irradiated sample of type (b) ⟨110⟩. Inverted empty triangle corresponds to a re-irradiated sample of type (f) ⟨149⟩.

by means of an empty triangle. In addition, the peak for a re-irradiated ⟨149⟩ sample (e in Table 1), plotted by means of an inverted empty triangle, is in good agreement in the Arrhenius plot too. Consequently, the LTP is consistent with a process of dislocation movement assisted by vacancy diffusion.

The microstructure of deformed ⟨110⟩ samples exhibits a more jogged structure than the ⟨149⟩ samples, in agreement with a larger quantity of slip systems activated during the tensile test in ⟨110⟩ samples, as it has been verified by TEM. In addition, we have found the evidence of the non-significant effect of the low flux neutron irradiation on the ⟨149⟩ samples. Therefore, the LTP relaxation can be related to the jog drag in the dislocation under movement, i.e., the LTP can be related with the dragging of jogs assisted by vacancy diffusion.

On the other hand, the HTP (around 1000 K) is not clearly affected by irradiation, but is related with the dislocations produced by the deformation of the samples. Peak intensity is also related to the number of slip systems activated by the plastic deformation in ⟨110⟩ and ⟨149⟩ samples and on the dislocation density. The high temperature and activation energy of this peak point to a process into which the vacancies are created and dragged by the dislocation movement. In fact, the self diffusion energy for vacancies, H_{sd}, can be written as the sum of the formation energy, H_{vf}, and migration energy, H_{vm} [37,38]. In addition, if the diffusion process is of type pipe diffusion, i.e. diffusion along the dislocation line, the activation energy, H_d, is related to H_{sd} through $H_d = a\,H_{sd}$, where a has values between 0.6 and 0.8, depending on the type of dislocation core [15,34–40]. In molybdenum, the reported values for H_{vm} and H_{vf} are among $1.35\ \text{eV} \leqslant H_{vm} \leqslant 1.60\ \text{eV}$ [41,42] and $3.0\ \text{eV} \leqslant H_{vf} \leqslant 3.2\ \text{eV}$ [42,43], respectively, leading thereof to H_{sd} between 4.35 and 4.8 eV. On assuming $a = 0.6$ [34,39,40], this leads to H_d values between 2.61 eV and 2.88 eV, which is in a reasonable agreement with the values of the activation energy measured for the HTP relaxation. Consequently, the HTP can be related to the formation and diffusion of vacancies assisted by the dislocation movement. In this case, vacancies can be produced and diffused at the core by the moving dislocations or by the movement of jogs. The type of mechanism associated to the HTP also explains that this peak in MS does not lead to a correspondent peak in the ER curve as it was in the case of the MS low temperature peak. For the LTP, vacancy type defects produced by deformation and/or irradiation move to dislocation at around 600 K producing ER changes (peak) and MS energy losses (peak) when the dislocation movements drag the vacancies. In the case of the high temperature peak there are no appreciable ER changes because no extra defects move (in this range of temperatures) to the dislocation to generate the MS high temperature peak. The movements of dislocation at these high temperatures are the ones that generate vacancy type defects producing the mechanical energy losses that can be detected in MS. In addition, it should be mentioned that although a peak in MS does not necessarily lead to a peak in ER curve, there exists a good correspondence between MS and ER results. Different characteristics of ER which appear at different temperatures correspond to salient changes which appear in the MS spectra.

On the other hand, the low neutron flux used in this work has been revealed to be very adequate to find out the origin of the relaxation peaks due to the high sensibility of the MS test. In fact, MS has been useful for detecting the movement of isolated interstitial atoms in bcc refractory metals in concentrations less than 10 atppm, during the stress-induced ordering, the so-called Snoek effect [15,44]. However, it should be emphasised that this present study involves the interaction of point defects (vacancies) with the dislocations. Indeed, the interaction of point defects with dislocations largely increased the intensity of the relaxation. Consequently, the possibility of being the physical effect studied even at very low concentration of point defects (less than 10 attpm) is easily achieved. For instance, the intensity of the peak related to the interaction of interstitials in niobium with dislocations, the so-called Snoek–Koester relaxation, can be larger by one order than that of the corresponding Snoek peak [45,46]. A damping peak of about 2×10^{-3} for the oxygen Snoek peak in niobium can lead to an oxygen Snoek–Koester damping peak of about 16×10^{-3}. Therefore, the concentration of vacancies which were estimated in our work, 5 atppm and 10 atppm for samples irradiated for 10 and 20 h, respectively, results in an affordable range during MS experiments when they are interacting with dislocations.

It is complicating to predict the response of the MS in irradiated samples at high fluxes since high fluxes will produce additional defects to the vacancy type defects we desired to obtain, as high density of dislocation prismatic loops and defect clusters [25]. Nevertheless, the effect of the irradiation at both higher doses and fluxes and also in temperature is an inalienable goal to extend this work, and it will be the aim of our future investigation.

5. Conclusions

Single crystalline deformed molybdenum exhibits relaxation peaks in the temperature range of about 0.3 Tm. It has been experimentally determined that the relaxations are two, each exhibiting one different driving force, although both involve the interaction of vacancies with dislocations.

The possible physical mechanism which controls the damping peak appearing at around 800 K (the LTP) can be related with the dragging of jogs by the dislocation under movement assisted by vacancy diffusion.

The damping peak which appears at higher temperatures of about 1000 K (the HTP) is more consistent with the formation and diffusion of vacancies assisted by the dislocation movement.

Acknowledgements

We acknowledge Professor J.N. Lomer for the interest in this present work and for the single crystal samples, B.A. Pentke for the preparation of samples for TEM and G.M. Zbihlei for the technical support during the TEM observations. We want also acknowledge Professor J.F. Ziegler for checking our handling of SRIM. This work was partially supported by the Collaboration Agreement between the Universidad del País Vasco and the Universidad Nacional de Rosario Res. CS.788/88-1792/2003, UPV224.310-14553/02 and Res. 3469/2007, the CONICET-PIP No. 5665 and the PID-UNR (ING 115) 2005–2007 and (ING 227) 2008–2009.

References

[1] J. Mazey, C.A. English, J. Less Common Met. 100 (1984) 385.
[2] S. Nemat Nasser, W. Guo, M. Liu, Scripta Mater. 40 (1999) 859.
[3] B. Mastel, L. Brimhall, Acta Metall. 13 (1965) 1109.
[4] L. Brimhall, B. Mastel, T.K. Bierlein, Acta Metall. 16 (1968) 781.
[5] R.C. Rau, J. Mottef, R.L. Ladd, J. Nucl. Mater. 40 (1971) 233.
[6] C.C. Matthai, D.J. Bacon, J. Nucl. Mater. 125 (1984) 138.
[7] J. Cornelis, P. de Meester, L. Stals, J. Nihoul, Phys. Status Solidi (a) 18 (1973) 515.
[8] A.S. Wrosnsky, A.A. Johnson, Philos. Mag. 213 (1963) 1067.
[9] H.B. Afman, Phys. Status Solidi (a) 13 (1972) 623.
[10] J. Nihoul, Symposium on Radiation Damage in Solids and Reactor Materials, vol. I, IAEA, Vienna, 1962. SM 25.
[11] G.L. Kulcinsky, H.E. Kissinger, Phys. Status Solidi (a) 2 (1970) 267.
[12] A.A. Johnson, J. Less Common Met. 2 (1960) 241.
[13] B.V. Cockeram, J.L. Hollembeck, L.L. Snead, J. Nucl. Mater. 324 (2004) 77.
[14] B.V. Cockeram, J.L. Hollembeck, L.L. Snead, J. Nucl. Mater. 336 (2005) 299.
[15] R. Schaller, G. Fantozzi, G. Gremaud (Eds.), Mechanical Spectroscopy, Trans Tech. Publ. Ltd., Switzerland, 2001.
[16] W. Benoit, in: R. Schaller, G. Fantozzi, G. Gremaud (Eds.), Mechanical Spectroscopy, Trans Tech. Publ. Ltd., Switzerland, 2001.
[17] A. Seeger, Philos. Mag. Lett. 83 (2003) 107.
[18] O.A. Lambri, G.I. Zelada-Lambri, L.M. Salvatierra, J.A. García, J.N. Lomer, Mater. Sci. Eng. A 370 (2004) 222.

[19] G.I. Zelada-Lambri, O.A. Lambri, J.A. García, J. Nucl. Mater. 353 (2006) 127.
[20] O.A. Lambri, Mater. Trans. JIM 35 (1994) 458.
[21] J.A. García, S. Hull, S. Messoloras, R.J. Stewart, J. Phys. E Sci. Instrum. 21 (1987) 466.
[22] T.S. Byun, M. Li, B.V. Cokeram, L.L. Snead, J. Nucl. Mater. 376 (2008) 240.
[23] G.H. Kinchin, R.S. Pease, Rep. Prog. Phys. 18 (1955) 1.
[24] J.R. Mathews, An introduction to thermomechanics including radiation effects, AERE – R13450, Harwell, 1989.
[25] H.C. González, A.M. Fortis, Radiation Damage, Multinational Project on Materials, AOS – CNEA, PMM/A – 155/94.
[26] J.F. Ziegler, J.P. Biersack, U. Littmark, The Stopping and Range of Ions in Solids, Pergamon, New York, 1985.
[27] D. Vesely, Philos. Mag. 27 (1972) 607.
[28] A. Luft, L. Kaun, Phys. Status Solidi 37 (1970) 781.
[29] V. Kopetskii, A.I. Pashkanskii, Phys. Status Solidi (a) 21 (1974) 741.
[30] A. Luft, L. Kaun, Phys. Status Solidi 18 (1973) 109.
[31] D. Vesely, Phys. Status Solidi 29 (1968) 685.
[32] H. Tanimoto, H. Mizubayashi, N. Teramae, S. Okuda, J. Alloy. Compd. 211/212 (1994) 54.
[33] H. Tanimoto, H. Mizubayashi, N. Teramae, S. Okuda, J. Alloy. Compd. 211/212 (1994) 136.
[34] J. Friedel, Dislocations, Pergamon, Oxford, 1967.
[35] O.A. Lambri, M. Massot, W. Riehemann, E.J. Lucioni, F. Plazaola, J.A. García, Phys. Status Solidi (a) 204 (2007) 1077.
[36] C.L. Matteo, O.A. Lambri, G.I. Zelada-Lambri, P.A. Sorichetti, J.A. García, J. Nucl. Mater. 377 (2008) 370.
[37] J. Philibert, Atoms Movements, Diffusion and Mass Transport in Solids, Monographies de Physique, Les editions de Physique, Les Ulis Cedex A, France, 1991.
[38] M. Koiwa, Mater. Trans. JIM 39 (1988) 1169.
[39] J. Cabané, in: J. Philibert, A.C.S. Sabioni, F. Dyment (Eds.), REM editora, Revista de Escola de Minas, Ouro Preto, Brasil, 1996.
[40] J.L. Bocquet, G. Brébec, Y. Limoge, in: R.W. Cahn, P. Haasen (Eds.), Physical Metallurgy, North-Holland Physics Pub., Amsterdam, 1983.
[41] M. Suezawa, H. Kimura, Philos. Mag. 28 (1973) 901.
[42] I.A. Schwirtlich, H. Schultz, Philos. Mag. A 42 (1980) 601.
[43] R. Ziegler, H.E. Schaefer, in: International Conference on Vacancy and Interstitials in Metals and Alloys, Berlin, September 1986.
[44] K. Schulze, E. Grallath, M. Weller, Z. Metallkunde 72 (1981) 439.
[45] B.J. Molinas, O.A. Lambri, M. Weller, J. Alloy. Compd. 211/212 (1994) 181.
[46] M. Weller, J. de Phys. C9 (Suppl. au 12) (1983) 63. tome 44.